

We are IntechOpen, the world's leading publisher of Open Access books Built by scientists, for scientists

4,800

Open access books available

122,000

International authors and editors

135M

Downloads

Our authors are among the

154

Countries delivered to

TOP 1%

most cited scientists

12.2%

Contributors from top 500 universities

**WEB OF SCIENCE™**Selection of our books indexed in the Book Citation Index
in Web of Science™ Core Collection (BKCI)

Interested in publishing with us?
Contact book.department@intechopen.com

Numbers displayed above are based on latest data collected.

For more information visit www.intechopen.com

Frameless Stereotaxy in Sheep – Neurosurgical and Imaging Techniques for Translational Stroke Research

Antje Dreyer^{1,2}, Albrecht Stroh³, Claudia Pösel¹,
Matthias Findeisen⁴, Teresa von Geymüller^{1,2},
Donald Lobsien⁵, Björn Nitzsche¹ and Johannes Boltze^{1,2}

¹*Fraunhofer Institute for Cell Therapy and Immunology,
Department of Cell Therapy, Leipzig,*

²*Translational Centre for Regenerative Medicine, University of Leipzig, Leipzig,*

³*Institute of Neuroscience, Technical University Munich, Munich,*

⁴*Institute of Analytical Chemistry, University of Leipzig, Leipzig,*

⁵*Department of Neuroradiology, University of Leipzig, Leipzig,
Germany*

1. Introduction

The continuous pathologic reduction of cerebral blood flow is mainly caused by thromboembolic occlusion of a brain-supplying artery or cerebral blood vessel disruption. These events, representing the most important causes for ischemic or hemorrhagic strokes respectively, lead to an acute breakdown of neuronal function, secondary brain damage by numerous mechanisms and the loss of cerebral tissue. In industrialized nations, stroke accounts for every third case of death. Cerebral stroke furthermore represents the most frequent reason for permanent disability in adulthood (Kolominsky-Rabas et al., 2006) and is therefore considered to be one of the most dreaded diseases from a clinical, socio-economic and individual, patient-related perspective.

1.1 Current state of the art clinical stroke treatment and diagnosis

Intravenous thrombolysis by tissue plasminogen activator (tPA) is currently the only FDA-approved, effective and potentially curative treatment (Blinzler et al., 2011) for ischemic stroke. However, this approach is restricted to a narrow time window of 4.5 hours (Hacke et al., 2008). The approach is further limited by a sharply increasing number needed to treat (Hacke et al., 2008; Lansberg et al., 2009) and a significant risk for fatal adverse events (Shobha et al., 2011) at later stages of this time window. As a result, more than 95% of all stroke patients do not significantly benefit from systemic thrombolytic treatment (Barber et al., 2001). Alternatively, endovascular thrombolysis under thorough radiological surveillance can be applied in specialized centers, extending the therapeutic time window to up to 8.0 hours under optimal conditions (Natarajan et al., 2009).

Cerebral ischemia needs to be discriminated from hemorrhagic stroke by means of magnetic resonance imaging (MRI) or computer tomography (CT) prior to the start of therapy, as inducing thrombolysis after hemorrhagic strokes is fatal. The mentioned imaging modalities are also used to monitor disease progression and the beneficial, or eventually detrimental, impact of any therapeutic intervention.

Even though intracerebral hemorrhages are treated by multimodal strategies including neurosurgical interventions and diligent monitoring of blood pressure (Flower & Smith, 2011), the event is still associated with high morbidity and mortality rates (Rymer, 2011), leaving about 80% of patients dead or disabled. Repeated patient surveys by MRI or CT is therefore pivotal for early detection of complications after hemorrhagic stroke. In summary, imaging procedures are of utmost clinical importance for diagnosis, treatment and onward care after ischemic and hemorrhagic strokes.

1.2 Current recommendations for preclinical stroke research

Preclinical and translational stroke research aims to overcome the aforementioned therapeutic and prognostic limitations by the development of novel treatment strategies. The application of stem cell based therapies is currently among the most promising approaches in the field (Burns & Steinberg, 2011) and the first clinical trials have already been initiated (Sahota & Savitz, 2011). However, despite thorough research, the development of novel stroke therapies is so far characterized by continuous setbacks and the general failure to translate promising findings from animal models into effective clinical treatment paradigms (Del Zoppo, 1995). In particular this holds true for the development of neuroprotective therapies (O'Collins et al., 2006).

The inability to translate preclinical findings into clinical therapies has been a matter of debate for more than 15 years. International expert committees like the "Stroke Treatment Academic and Industry Roundtable" (STAIR) and "Stem Cell Therapies as an Emerging Paradigm in Stroke" (STEPS) consortia were formed to define, discuss and publish recommendations for adequate preclinical stroke research (The STAIR Participants, 1999; The STEPS Participants, 2009). Current guidelines for state of the art assessment of novel stroke treatment strategies comprise the design and application of relevant animal models (Fisher et al., 2009), the definition of the optimal route of administration for any therapeutic agent (Savitz et al., 2011; The STAIR Participants, 1999), as well as the choice of relevant imaging protocols to monitor therapeutic safety and efficacy (Savitz et al., 2011).

1.3 The role of large animal models in translational stroke research

Cerebral ischemia is mainly modeled by transient or permanent occlusion of the middle cerebral artery (MCA; Howells et al., 2010). Rodent models are widely available and represent experimental key systems for preclinical stroke research. These models offer many advantages such as well established methodology including surgical techniques, imaging procedures, histological techniques and protocols for molecular biology. Further, the availability of genetically modified strains and excellent tools to assess functional outcome favor the use of rodent stroke models.

However, the impact of a particular therapy in the gyrencephalic brain can only be assessed in large animals. Therefore, the use of a second, predominantly large animal species has been recommended by the STAIR and STEPS committees. Existing large animal models include rabbit (Amiridze et al., 2009), canine (Kang et al., 2007), feline (Garcia et al., 1977),

and porcine (Imai et al., 2006) models for which middle cerebral artery occlusion (MCAO) techniques have been described. For anatomical reasons, most large animal models require enucleation and show high mortality rates (The STAIR Participants, 1999), rendering their applicability for long term safety and efficacy trials difficult.

Early models of cerebral hemorrhage were reported more than 45 years ago (Klintworth, 1965), using the application of mechanical force (e.g. balloon inflation) to induce cerebral hemorrhages. More contemporary models are often based on atlas-guided stereotaxic injections (Bullock et al., 1984) of autologous blood or bacterial collagenase into cerebral tissue, predominantly the rodent striatum (MacLellan et al., 2010). MR-guided application techniques have recently been reported in primates (Zhu et al., 2011) but are rarely used, presumable due to ethical and financial restrictions.

1.4 The ovine stroke model and its use for preclinical research

To compensate the above mentioned common limitations of large animal models an ovine model of ischemic stroke using permanent MCAO was developed by our group (Boltze et al. 2008). This model avoids enucleation and allows for long term observation of subjects due to minimal mortality rates.

Briefly, the method can be described as follows. A transcranial access is performed between the left eye and ear. Animals should be placed on the right side to avoid ventilation insufficiency due to a gaseous rumen edema during surgery. After superficial shaving and disinfection, the temporal muscle is incised at the Linea temporalis and temporally elevated from the parietal skull bone. Then, a trepanation of about 1 x 1 cm is performed right behind the orbital rim. After careful incision of the dura mater, the MCA is permanently electrocoagulated by a bipolar forceps. Occlusion of either one or two MCA branches or the entire cortical vessel allows a detailed control of lesion size and functional deficits (Boltze et al., 2008). The drill hole may be sealed by sterile bone cement after suturing of the dura. However, leaving the craniotomy open (only covered by the temporal muscle) avoids pathophysiological increase of intracerebral pressure in early post-stroke phases, significantly reducing post-stroke mortality. After refixation of the temporal muscle at the Linea temporalis and suturing the skin wound, the animals can be taken back to the stable and are allowed to recover. Adequate post stroke analgetic and antibiotic treatment has to be ensured. For any details regarding animal medication, behavioral phenotyping, advanced imaging and the surgical procedure itself, please refer to Boltze et al. (2008).

Species-appropriate housing can be realized with comparatively low efforts and over extended time periods. The price per sheep is relatively low and the species is broadly available. A special feature of the sheep stroke model is the control of lesion size and subsequent behavioral deficits by occlusion of the cortical MCA or a defined number of its branches. A protocol for testing and quantification of neurological functions is available to assess the impact of the MCAO modality and a potential therapeutic procedure. Moreover, the model is eligible for detailed MR, CT and positron emission tomography (PET) studies as well as the assessment of autologous cell therapies.

2. Stereotaxy and cell tracking for stroke-related applications

Stereotaxic concepts were developed as minimally invasive surgical approaches which use three-dimensional Cartesian or polar coordinate systems to localize small targets inside the

body. The approach can be used for both diagnostic and therapeutic applications, as it allows the placement or the removal of a specimen from a certain location within the body with highest precision and minimal damage to the surrounding tissue. Stereotaxy is of particular importance in neurosurgery where the technique is routinely used for diagnosis and treatment of intracranial tumors (Willems et al., 2006), as well as for the application of deep brain stimulation electrodes in Parkinson's disease (Starr et al., 1998) and neuropathic pain (Stadler et al., 2011). The fibrinolytic evacuation of intracranial hemorrhages by a stereotaxic approach has also been reported (Samadani & Rohde, 2009). Moreover, stereotaxic stem cell injections into the human brain are used in phase I and II clinical trials, as the local administration of therapeutic compounds close to the lesion is considered to be advantageous.

Albeit these concepts may have been strongly perpetuated towards clinical application clinical trials during the last years; the first reported results unfortunately resemble the translational failures that were known from past efforts. This holds true for experimental treatments in the field of stroke (Kondziolka et al., 2005) and Parkinson's disease (Gross et al., 2011) although these concepts were positively evaluated in preceding rodent studies. This emphasizes the relevance of large animal models as an important translational milestone. Whereas simplified stereotaxic devices based on brain atlases are widely available for rodents, the accuracy and complexity of human stereotaxic devices can currently only be modeled in primates. However, this complexity, including the individual, "lesion-specific" application of substances or the induction of phenotypically varying intracerebral hematomas may be critically needed in translational research to mimic the more heterogenic patient populations enrolled in clinical trials.

We expanded the sheep model to fill this methodological gap and to provide an additional large animal model for translational research in cell transplantation after ischemic stroke and intracerebral hemorrhages. Our model allows precise, MR-guided implantation of magnetically labeled, bone-marrow derived mesenchymal stem cells (stroke treatment) and autologous blood samples into the ovine brain (hemorrhage induction). The technique was developed using the Brainsight™ neuronavigation system (Rogue Research Inc., Quebec, Canada) and several modifications were applied to adapt the system to the ovine skull anatomy. Cell tracking can be performed reliably using clinical MR scanners with adequate resolution and sensitivity.

This chapter describes the methodology of image-guided frameless stereotaxic surgery in sheep with special emphasis on (i) the application of an autologous therapeutic cell population (e.g., the mesenchymal stem cells), (ii) the previous labeling and subsequent imaging protocols for MR-based cell tracking in sheep and (iii) the MR-guided induction of cerebral hemorrhage in the species.

3. Technical description of surgery

3.1 General information about the species and handling requirements

The neurosurgical approach for stereotaxy in sheep requires hornless subjects for easy accessibility of cranial structures. Merino sheep may be of advantage as many hornless strains can be found in this widely available race. Adult merino sheep weigh approximately 80 kilograms (ewe) to 130 kilograms (rams) and have a wither height of about 0.9 meter. This body size allows for relatively easy handling. Frequent and early contact to humans facilitates familiarization and improves the handling. Species appropriate housing, feeding

as well as thorough medical inspections and blood screening, medication and vaccination ensure a significant reduction of postoperative complications and thereby enhance study quality (Boltze et al., 2008).

Anesthesia is performed as described elsewhere (Boltze et al., 2008). Animals should be intubated after induction of anesthesia and placed in a prone (“sphinx”) position during surgery and imaging. Vital parameters (electrocardiogram, oxygen saturation, blood pressure, rectal body temperature) should be continuously monitored during any surgical intervention.

3.2 Frameless stereotaxy in sheep – preparation and data acquisition

The neuronavigation device, BrainSight™, is a frameless system that allows for MRI data set based planning of surgical approaches as well as for surveillance and precision control of the surgical intervention with an optical position sensor (Frey et al., 2004). An individual 3D-reconstruction of the head, especially the brain, is required for the precise planning and performance of the stereotaxic injections.

3.2.1 Fiducial marker positioning and imaging

The MR-compatible fiducial markers are attached to a maxillary splint (Fig. 1a). The use of the splint is different from neurosurgical approaches in human medicine, where fiducial markers can be fixed directly to cranial bones. This is not recommended in animals due to safety and welfare issues, especially when the animal is awake between MRI data set acquisition and surgery. The maxillary splint consists of a mouthpiece (Fig. 1a, 1) and two angled arms (Fig. 1a/b, 2) that hold the fiducial markers (Fig. 1a/b, 4). The mouthpiece is inserted carefully, avoiding damage to or constriction of the tracheal tube. It can be adapted to the individual shapes of the maxillary molars and the hard palate by using thermoplastic, which cures within a few minutes. The fiducial markers are usually placed in the area between the cheeks and the ears. The maxillary splint has to be adapted to each individual sheep to ensure maximum precision. The splint has to be inserted for imaging and surgery.



Fig. 1. Maxillary splint with fiducial marker

a) maxillary splint with mouthpiece (1), angled arms (2), bar spacer to the skin (3) and fiducial marker (4); b) sheep before surgery, the maxillary splint is inserted and fixed with a bandage. The angled arms (2) support the fiducial markers (4); c) 3D-MRI reconstruction of the skin illustrates the position of fiducial markers between cheek and ear (black arrow heads)

It should be fixed with bandages to ensure an accurate, stable and reproducible position. Otherwise, even minor displacements of the fiducial markers may lead to large divergences between planned and realized target.

A 1.5 T scanner is sufficient for MRI data set acquisition even though the use of a 3 T scanner is recommended. The optimal time span between data acquisition and surgery should be long enough for animal recovery from imaging anesthesia. However, for cell transplantation after MCAO, this time span must not be too long to stay within a potential therapeutic time window. Usually, a recovery phase of one day is sufficient, but longer recovery phases should be scheduled if permitted by the experimental design.

After initial anesthesia and transport, the sheep is placed on the scanner table and is fixed using adhesive tape (cloth tape tesa®, Tesa SE, Hamburg, Germany) on shoulder and hip, which can be easily removed from the wool. The sheep is covered by a drape which offers limited protection from cooling and prevents soiling of the scanner. For subsequent target planning, a high-resolution T1-weighted 3D sequence is acquired with a minimum resolution of 1 x 1 x 1 mm. Acquisition time depends on the number of averages, but usually does not exceed 30 minutes. Additionally, an acquisition of an angiographic sequence is recommended in order to avoid damaging major intracerebral vessels during surgery (see paragraph 3.2.2).

3.2.2 Planning of surgery

The BrainSight™ software (V2.1) consists of a graphical user interface with a tab based arrangement of modules (Fig. 2a, red rectangle). Pre-surgical image processing includes several steps that are explained in detail in the following paragraph.

After starting the software, the MRI data set has to be loaded. Therefore, click of the “Anatomical” tab (Fig. 2a, 1):

1. Select MRI 3D data set by pressing “Choose” and load the data.
2. Identify positioning of animal by clicking on “Show Image & Detail” (Fig. 2a, 2).
3. Choose the radio button which corresponds to the correct animal position (e.g. “actual” orientation → Sphinx Heads First; “scanner” orientation → supine head first)

To avoid accidental intrasurgical damage of major cerebral arteries, an overlay with an angiographic data set is recommended. Therefore, use the “Overlays” tab:

1. Implement the data set by clicking “Load Overlay”.
2. Define the desired opacity by choosing the corresponding slider.

In the next step, anatomical structures can be defined by segmentation. While the skin reconstruction is performed automatically, other relevant anatomical structures like the brain and cranial bones have to be identified separately and on each slice. Select the “ROIs” (=region of interest) tab to perform this operation:

1. Press “New ROI from Region Paint”.
2. Name the ROI (e.g. “brain”).
3. Choose a threshold of grey value to localize the structure by moving the slider (Fig. 2b, 3).
4. The opacity of the selection can be changed by the corresponding slider (Fig. 2b, 4).
5. Start segmentation of the threshold areas in the middle of the brain by pressing on the “Seed Tool” icon (Fig. 2b, 5) and select the threshold area of the brain.
6. If necessary, correct the segmentation manually using the “Erase pencil”. Cut the unwanted conjunction between target and non-target structures and clear all non-target structures using the “Erase Fill” tool (Fig. 2b, 5).

7. Choose the next slice.
8. Repeat points 5 to 7 for each MRI slice until all areas of the specific structure are completely selected.
9. Repeat steps 1 to 8 for any other target (e.g. bone, see below).

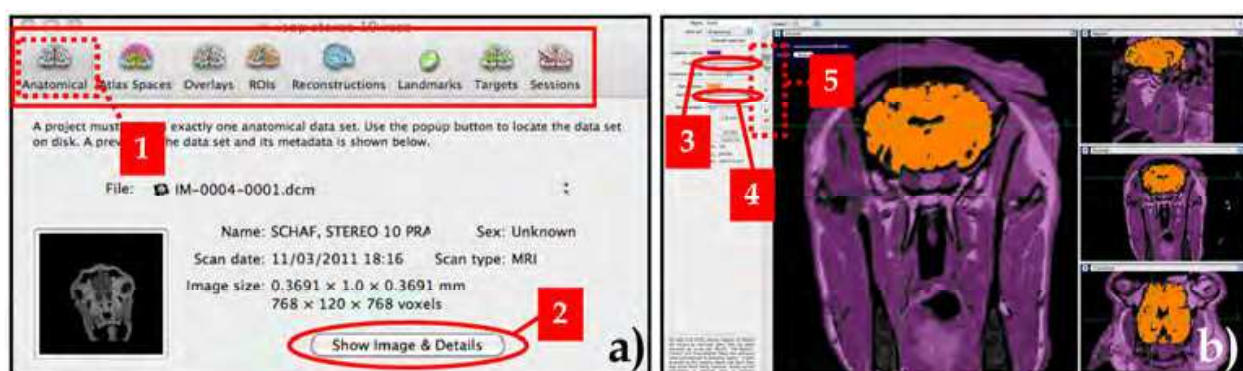


Fig. 2. BrainSight™ software applications I

a) Graphical user interface with tab based modules (red rectangle), “Anatomical” tab (1), “Show Image & Detail” button (2); b) “ROIs”: reconstruction of the brain from MRI data set, slider of grey value threshold (3), slider of opacity (4), icon tools (5)

3D reconstructions are created after defining the ROIs. A skin reconstruction is necessary to register the fiducial markers. It is recommended to render 3D reconstructions from brain and bone. Use the “Reconstruction” tab as follows:

1. Skin reconstruction is performed automatically by choosing “Surface Skin”. Use the threshold slider to suppress inclusion of air and/or wool in the skin rendering. Press “Compute skin” and subsequently name the reconstruction (e.g. “skin”).
2. Bone and brain are calculated by selecting “Surface from ROIs”. Label the generated surface as “bone” and “brain”. Choose corresponding ROI from the “Select button” and press “Compute Surface”.

The MRI-positive fiducial markers need to be relocalized manually in the MRI data set. The tagging of these pivotal landmarks requires maximum precision. Use the “Landmarks” tab:

1. Switch the layout to “1 | 3 windows”.
2. Skin surface reconstruction should be opened in the large left window by choosing “Skin” of the select button (Fig. 3a, 1).
3. MRI data sets are now opened in three windows on the right side. Select “Inline & All Landmarks” in the upper, “Inline 90 & All Landmarks” in the middle and “Perpendicular & All landmarks” in the bottom window. You may wish to zoom out the fiducial marker for better view of their position.
4. Choose “sphere” from the select button (Fig. 3a, 2) as the shape of the fiducial markers. Coordinate system is “Brainsight” (preselected).
5. Press “New” (Fig. 3a, 3). The compiled landmarks will be named automatically.
6. Select a landmark position by choosing a fiducial marker in the skin reconstruction. It will be marked with a sphere. The crosshair in the MRI data now indicates the corresponding position in all views. Correct the relative position of the fiducial marker in each view using the sliders on the right hand side of the screen (Fig. 3a, 4). Position the cursor so that the crosshairs perfectly represents the middle of the fiducial marker in

the upper “Inline & All Landmark” frame and the “Inline 90 & All Landmarks” using the using the “AP” (anterior/posterior) and the “Lat” (medial/lateral) slider.

7. Press “New” for a new landmark and repeat step 6 until all fiducial markers are identified as landmarks by the software.

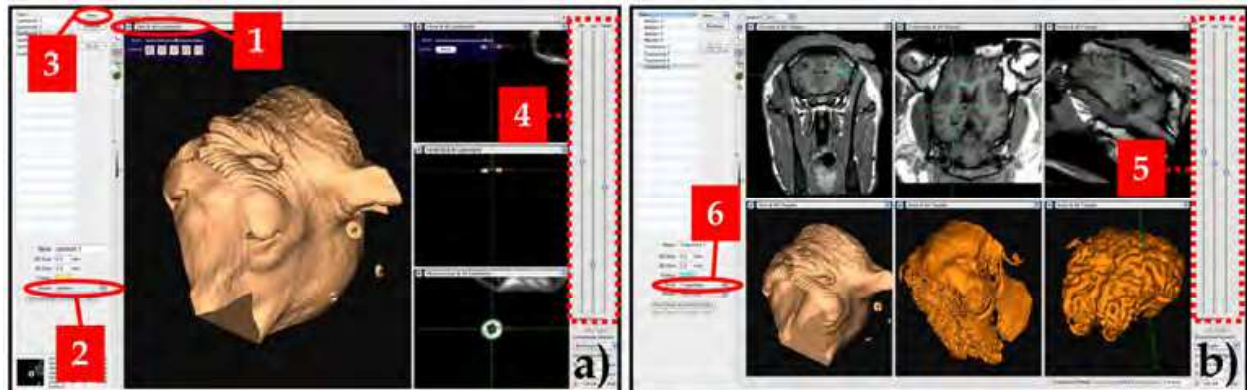


Fig. 3. BrainSight™ software applications II

a) identification of landmarks by MR images using the “landmarks” tab, select button of window view (1), select button of the shape of the fiducial marker (2), “New” button (3), sliders for positioning (4); b) definition of targets and trajectories in MRI and 3D reconstructions of skin, bone and brain, sliders for positioning (5), select button of marker or trajectory (6)

The last step of the planning procedure is the identification of the surgical targets according to the study design. In addition, optimal trajectories are planned during this step. The following recommendations for accessing the target should be considered to ensure a minimal invasive surgical procedure and to avoid surgical problems and complications:

- i. Avoid the perforation of the horn plate, even hornless animals have one.
- ii. Avoid the perforation of the frontal sinus.
- iii. Avoid a trajectory that crosses major vessels (as identified by the angiographic overlay).
- iv. Avoid cerebral sulci.

The route to the target (trajectory) and the target itself (marker) should be defined as follows using the “Targets” tab:

1. Switch to a 2 x 3 layout and arrange the frames as follows: MRI data are shown in the upper row and the reconstructed objects in the bottom row. Select “Coronal & All Targets” in the 1st, “Inline 90 & All Targets” in the 2nd and “Inline & All Targets” in the 3rd upper frame. Select “Skin & All Targets”, “Bone & All Targets” and “Brain & All Targets” in the bottom row.
2. Coordinate system is “Brainsight” (preselected).
3. Place the crosshair at your target (since a homogeneous MRI signal from the target structure is preferred for the cell tracking experiments, the Corona radiata was used in this example).
4. Use the sliders (Fig. 3b, 5) to place the trajectory (arrow in the crosshair) and make sure it is chosen with respect to the aforementioned recommendations. Ascertain the position of the trajectory in each frame and correct the access using the “AP”, “Lat” (lateral) and “Twist” sliders.
5. Choose “Trajectory” in the select button (Fig. 3b, 6) to confirm the planned trajectory. The trajectory is named automatically.

6. Choose "Marker" from the select button ("New" is preselect) to define the target point. The marker is named automatically.
 7. Repeat steps 3 to 6 for more trajectories and markers.
- Finally, the project should be saved to a specified folder (Menue → "File").

3.3 Frameless stereotaxy in sheep – surgical procedure

3.3.1 General surgery

The Brainsight™ hardware comprises an optical position sensor and a number of surgical devices (Fig. 4). During surgery the anesthetized sheep is placed in the prone position on the

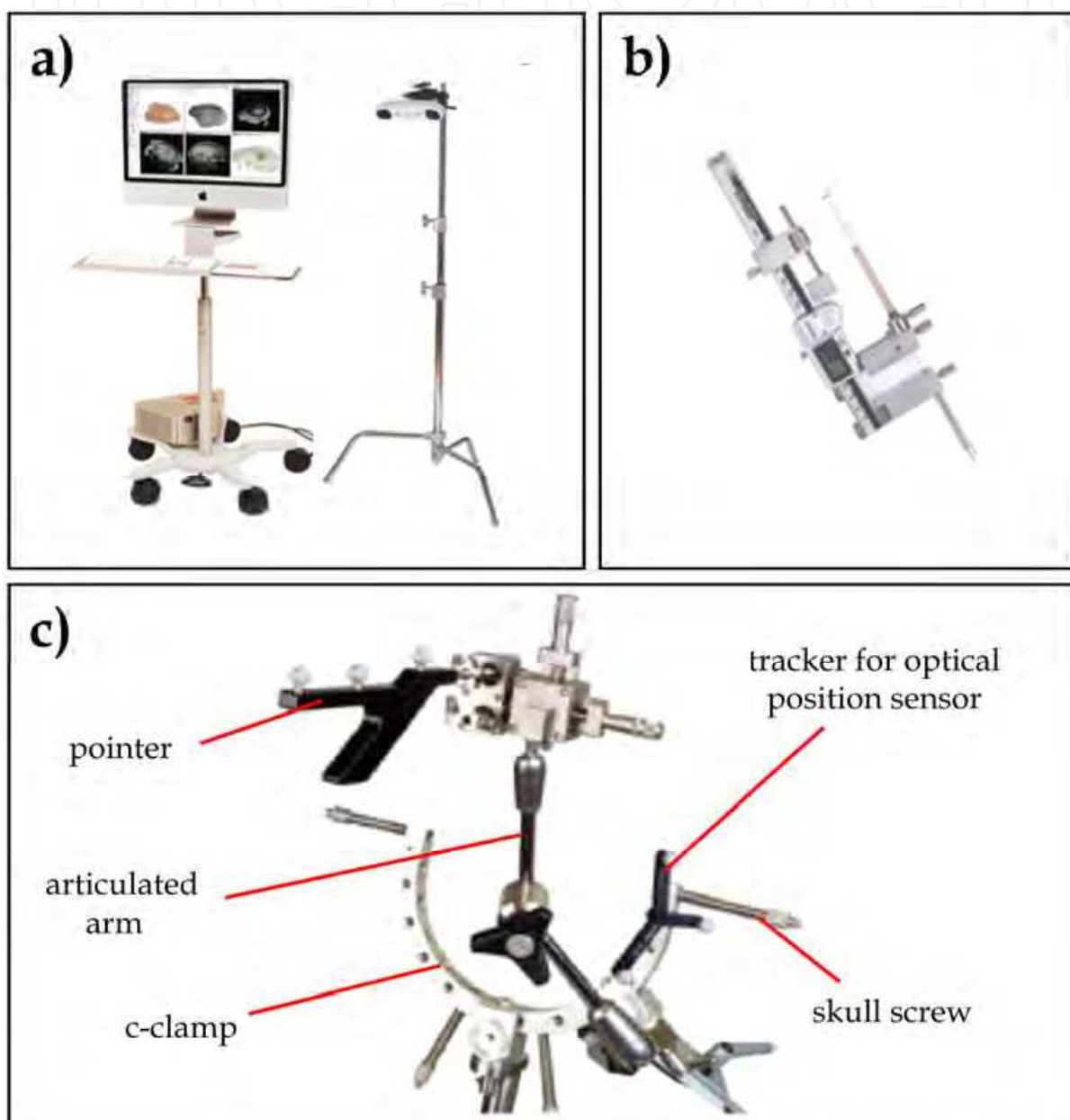


Fig. 4. Brainsight™ hardware

a) The peripheral hardware of Brainsight™ system comprises a computer and an optical position sensor (Polaris®); b) Additionally, a drill guide (not shown) and a ruler guide are available on request; c) The surgical instruments and hardware

operating table. On smaller tables, fix the animal with adhesive tape in the shoulder and hip region. The head rests on a foam rubber pad to ensure a stable and correct position. The upper head of the animal needs to be shaved and disinfected. Next, the maxillary splint has to be placed precisely in the mouth (ensure its correct position) and it should be fastened tightly with a bandage.

A rigid half-circular clamp (c-clamp) is used for fixation of the head and to provide support for the articulated arm. A similar holder system with skull pins is also used for neurosurgical procedures in humans (Olivier & Bertrand, 1983). The c-clamp is fixed to the skull bone by at least four adjustable skull screws. To avoid skull damage the screws are positioned at distinctive spots (e.g. beneath the Linea temporalis and ventral of the Protuberantia occipitalis externa, Fig. 6a). After fixing the c-clamp to the skull, the whole assembly is attached to the operating table using the adjustable mounting system. The system allows to lock the c-clamp, and thereby the skull in the appropriate position. Next the articulated arm is mounted at the c-clamp. Ensure that the entire field of surgery can be reached by the arm. Thereafter, the tracker (containing three track balls which can be recognized by the optical position sensor) is positioned at the c-clamp to act as a fixed optical reference for the coordination system. The system is now ready for merging the virtual MRI data with the spatial position of the sheep's head. The previously processed data sets (MR images, predefined landmarks and targets) have to be reopened by using the "File" option ("Open Project") in the menu. Choose the "Session" tab:

1. Choose "New Online Session" from the select button.
2. Select all "Targets in project" in the opened frame and move them to "Targets to sample in this session" via the drag and drop operations.
3. Press "Next Step" to enter the "Polaris" submodule in the "Session". A new frame will be opened automatically.

Next, the Polaris® optical position sensor has to be configured and adjusted:

1. Make sure the "Polaris status" is "ok" (Fig. 5a, 1) and that all tools (pointer, subject tracker) are located in the detection space (visible field). Otherwise press "Reset Polaris".
2. The tracker (fixed to the c-clamp) should be placed in the middle of the visible field by moving the Polaris camera. Ensure the correct position of the subject tracker in 3D, top, lateral and frontal view. Make sure that the visible field is wide enough to track the pointer when navigating in the periphery of the head. To check this move the Pointer in the 3D field of view).
3. Press "Next Step" (Fig. 5a, 2) to enter the "Registration" module.

Next steps require the spatial allocation of the surgical object (head) and MR images. Therefore, the registration of (physical) fiducial markers with the already defined virtual landmarks is performed as follows:

1. Switch the layout to 1|3 windows and use the same window allocation as during landmark tagging.
2. Perform manual registration update.
3. Select one landmark from the list. The correct selection will be confirmed acoustically. The specific landmark is now displayed and marked in each window.
4. Place the tip of the pointer in the divot of the corresponding fiducial marker. This is the most important step to ensure precision of the surgical approach. The pointer has to be placed orthogonally to the divot in each dimension. Avoid any pressure on the fiducial marker, which may alter its position. Make sure the pointer can be detected by the

optical position sensor. Make sure that the pointer does not move when recording the location of a fiducial markers.

5. Press “Sample & Go to next landmark”.
6. Repeat Point 3 to 5 until all landmarks are co-registered with the fiducial markers.
7. Press “Next Step” to enter “Validation” procedure of the registration (see below).

The allocation of the landmarks and fiducial makers is validated as follows:

1. Arrange a 2 x 3 layout.
2. Place the pointer randomly in the divot of each fiducial marker. After ideal co-registration, the pointer tip should now precisely indicate the corresponding landmark. Check the distance of the pointer tip to the corresponding landmark. A vector drift of 1.6 mm can be tolerated, but a difference of <1.0 mm is strongly recommended while a deviation of <0.6 mm is optimal. Repeat the “Registration” in the case of >1.6 mm vector deviation or to ensure demanded precision.
3. To check for lateral deviation in registration of the subject’s head, place the pointer on the skin surface at a virtual line between the eyes. Three points per side are recommended. Control the distance in the “Coronal” view, in the “Inline” view and in the “Skin” reconstruction. Repeat the registration in case a unilateral shift is noticed.
4. For longitudinal deviation, place the pointer at several points on the skin (six are recommended) in the midline of the cranium. Control the distance in the “Sagittal” view, in the “Inline” view and in the “Skin” reconstruction. Repeat the registration in case of a dorsoventral shift. NOTE: Skin thickness may be altered due to the animal being fixed in the c-clamp, causing the occipital skin to be pulled tautly or to bulge. This may alter the preceived skin thickness.
5. Press “Next Step” to continue with planning the surgery.

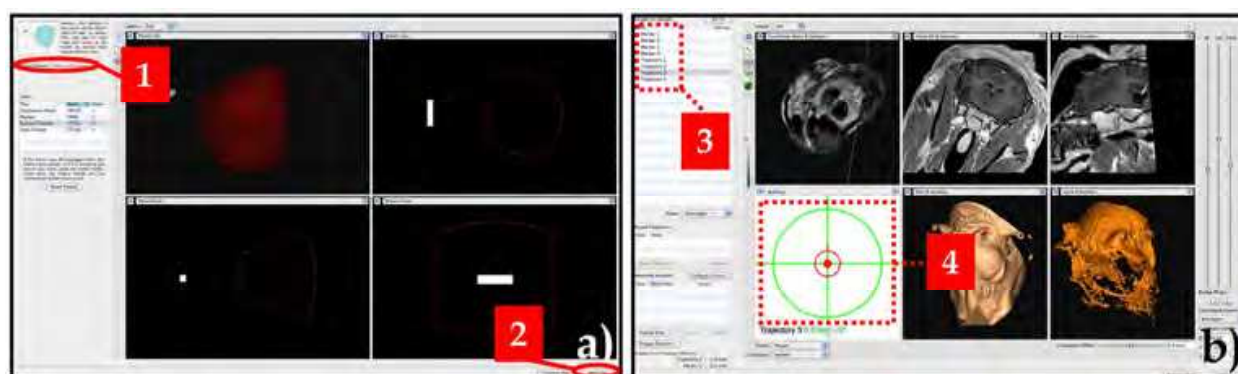


Fig. 5. BrainSight™ software applications III

a) Screenshots taken during the setting of the Polaris® optical position sensor. The tracker and the moveable pointer have to be located in the 3D field. Polaris status (1), “Next Step” button (2); b) For adjustment of trajectory and target (3) within the “Session” tab, the red “Bullseye” (4) has to overlap with the green crosshair as shown

Following this step, adjust the surgical access and the targets. Recall the planned targets in the software interface:

1. Arrange a 2 x 3 layout as follows: upper row comprises “Coronal & samples”, “Inline 90 & samples” and “Inline & samples”. Bottom row contains “Bullseye”, “Skin & samples” and “Bone & samples”.

2. Check that the coordinate system is “Brainsight”, driver is “Pointer”, and Crosshair is “Needle”.
3. Select the first trajectory (Fig. 5b, 3).
4. Place the pointer in the articulated arm for adjustment of the trajectory (Fig. 6b). The pointer represents the needle to be inserted during surgery. Make sure the pointer is both locked in the chuck and located in the visible field.
5. Place the pointer tip next to the expected surgical access (drill hole) position by moving the articulated arm. After approximate adjustment, ascertain that the “Bullseye” (red circle) overlaps with the green crosshair.
6. Use the x-y stage to optimize the position. Make sure the red dot of the “Bullseye” aligns with the crosshair (Fig. 5b, 4).
7. Lock the articulated arm and place the stabilizing pin in the guide. Ensure that all hardware pieces are in the correct position and tightly locked now.
8. Measure the thickness of the cranial bone at the level of access in the “Inline 90 & samples” view on the computer. In order to avoid damage to the dura mater or the brain by drilling to deep you may wish to underestimate bone thickness by 0.5 mm.

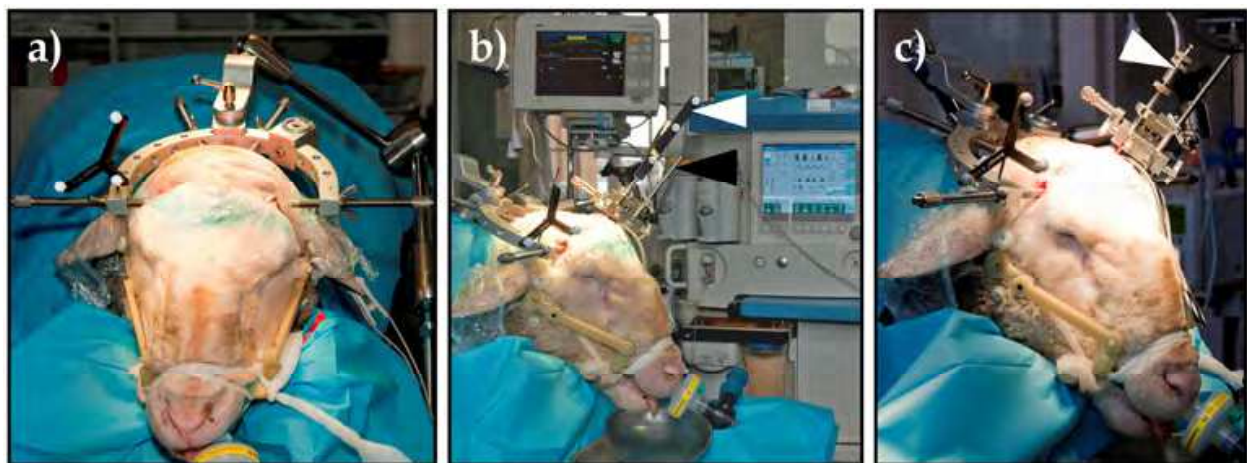


Fig. 6. Surgical set-up in sheep

a) Position of the c-clamp, fixed with 4 skull screws beneath the Linea temporalis and Protuberantia occipitalis externa, note the tracker on the right side of the c-clamp; b) The articulated arm is mounted on the c-clamp and additionally fixed by a sharp stabilizing pin (black arrow). The pointer (white arrow) is placed in the articulated arm at the desired trajectory. c) Drill guide (white arrow) for manual drilling is placed in the arm (Please note that the subject's head is not covered by surgical drape for better illustration)

The skin above the desired access is locally incised. The incision usually does not exceed one centimeter. The periosteum is removed using a Willigers raspatory. You may use small retractors for better accessibility. For skull trepanation, adjust the drill guide to the measured bone thickness, mount it at the end of the articulated arm and place it directly on the exposed skull surface. Drilling is performed at lower speed (10,000 rpm or less, for example using a Microspeed® uni, Aesculap AG, Tuttlingen, Germany). Since minor deviation between measured and real bone thickness can occur, the dura mater may not be reached after drilling. In that case, carefully continue with manual drilling (Fig. 6c). The correct position of the drill hole within the planned trajectory should be checked by placing

the pointer tip in the drill hole. In case of minor deviation, the drill hole can be easily expanded during this step.

Next, the distance from the drill hole to the intracerebral target must be measured. Place the pointer tip in the drill hole at the level of the skull surface, not the level of the dura. The distance between the pointer tip and the target should now be displayed on the computer. Thereafter, a ruler guide with digital display is placed in the articulated arm. The instrument to be inserted into the brain, for example a filled Hamilton syringe (see 3.3.2), is mounted at the ruler guide. The tip of the instrument (e.g. a syringe cannula, Hamilton Company USA, Reno, USA) has to be positioned at the level of the skull surface, as done with the pointer tip for distance measuring. Now, set the digital display to zero for reference. The cannula can be inserted to the desired depth (Fig. 7).

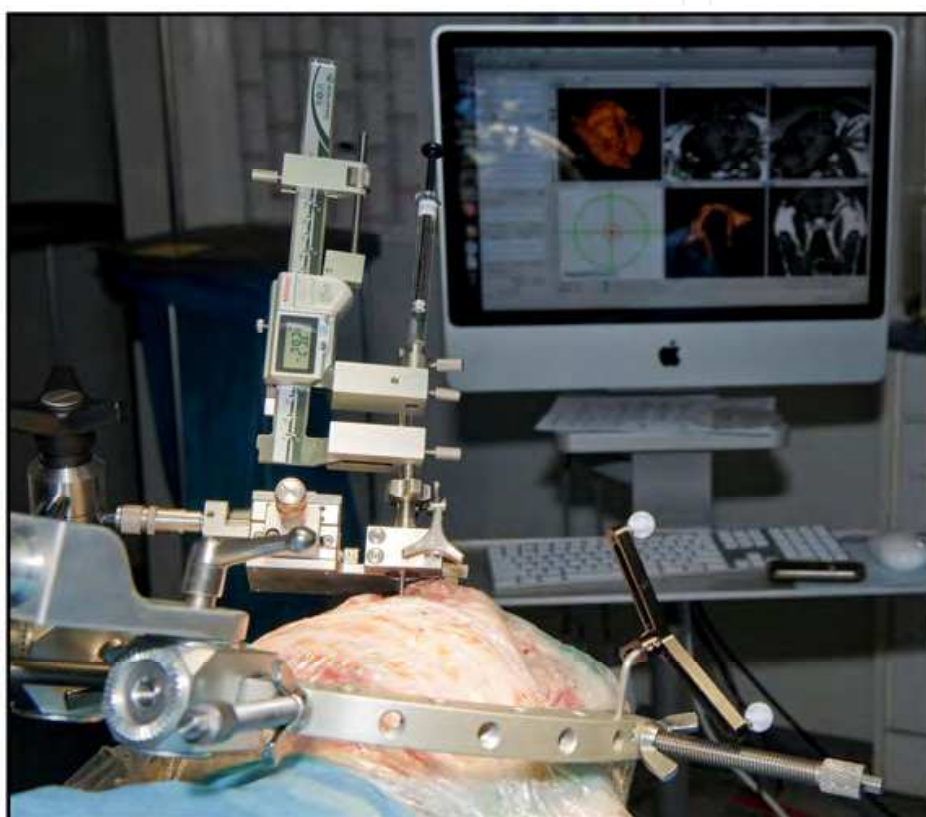


Fig. 7. Application equipment with ruler guide and Hamilton syringe. The syringe is inserted to a depth of 29.2 mm in the given example.

This should be done in a slow and steady manner to avoid microbleedings and injuries. Do not advance faster than 2 mm per minute. In case you want to inject any kind of substance or cell solution (as in the example given in 3.3.2) this should also be done slowly, ideally using a micropump at a maximum pump rate of 5 μ l per minute. The cannula is left in position for another ten minutes to allow the injected substance to diffuse locally. The explantation of the cannula is done according to the implantation. Repeat all steps above for multiple insertions. Verify the trajectory for each individual injection. At the end of the surgery, the drill hole is plugged with sterile bone wax, the articulated arm and the c-clamp are removed carefully by detaching the screws, and the skin wounds are sutured. Before the animal awakes from the anesthesia, the maxillary splint is carefully removed and the sheep receives postoperative medication with antibiotics and analgesics for 5 days.

3.3.2 Exemplary applications

Exemplary application for stereotactically guided (cell or blood) depositions following stroke and other cerebral disorders are an emerging field of research in regenerative medicine. This route of administration is expected to be used in upcoming clinical trials. The sheep model allows the simulation of autologous cell therapies, in particular using intracerebral stereotactic cell delivery. This may be required for example when cell depots need to be placed next to a lesion site, which may vary between individual cases.

In the described stereotactic model, autologous bone marrow stromal cells (BMSC) were chosen as an example since these cells were reported to be beneficial after stroke treatment and neurodegenerative diseases (Joyce et al., 2010). Also other cell types like neural or embryonic stem cells were used for local transplantation close to the infarcted area border (Guzman et al., 2007) or into the contralateral hemisphere (Hoehn et al., 2002) in rodent models. After purification and cultivation (see 4.1.1), a defined cell number is suspended and stored in a Hamilton syringe with a 15.6 cm long cannula. The technique of stereotactic transplantation is described in 3.3.1. For post-translational tracking, the cells can be labeled with iron oxide nanoparticles such as VSOP (very small superparamagnetic ironoxide particles, Ferropharm, Germany) (see 4.1.1). The localization and migration of transplanted cells is monitored by MRI (see 4.1.2).

Alternatively, the stereotactic device can be used to model cerebral hemorrhage by application of blood into the sheep brain. For that purpose, autologous blood is collected from an arterial (preferred) or venous line in a heparinized syringe and is transferred to a Hamilton syringe before application. The steps are technically identical with the injection of cells (see 3.3.1). The injected blood volume depends on the planned region and the target dimensions, but should not exceed two milliliters in sheep (approx. weight of sheep brain: 120 g).

4. Application examples

4.1 Concept 1: Cell labeling for MRI-based tracking in vivo

4.1.1 Harvesting and processing of Bone Marrow Stromal Cells (BMSC)

Autologous cell harvest and cell processing

BMSC are commonly isolated from bone marrow aspirates. Bone marrow samples may be harvested from the iliac crest in humans and in sheep. Therefore, the puncture area on both iliac crests are shaved and disinfected while the anesthetized sheep is placed in a prone position. Samples of approximately 10 mL of bone marrow are taken from both sides by multiple punctures using a heparinized syringe. Higher aspiration volumes from single punctures may result in contamination with peripheral blood. In the next step, the mononuclear cells (MNC) are isolated by density gradient centrifugation, which should be done within one hour after bone marrow harvest. A protocol for the separation of ovine MNC is stated below.

1. Dilute bone marrow with phosphate buffer saline (PBS, Biochrom KG seromed®, Berlin, Germany) at a 1:1 (v/v) ratio.
2. Merge Biocoll (1.077 g/mL, Biochrom KG seromed®, Berlin, Germany) and Pancoll (1.091 g/mL, PAN-Biotech GmbH, Aidenbach, Germany) in a ratio of 1:1 (v/v) to obtain a density of 1.084 g/mL (separation medium). Add 7 mL of mixed separation medium into a 50 mL falcon tube.
3. Carefully place a layer of 10 mL of diluted bone marrow onto the gradient mixture. Avoid commixture between cell layer and the separation medium.

4. Centrifuge at 1,000 x g for 25 min.
5. Carefully transfer the interface layer of mononuclear cells to a sterile centrifuge tube by using a sterile pipette (Fig. 8a).
6. Wash cells twice in PBS.
7. Count MNC.

The BMSC population is isolated from MNC based on its ability to adhere to the cell culture flask. For that reason, MNC are seeded at a density of $5 \times 10^4/\text{cm}^2$ in a culture flask. Cells are cultivated with DMEM (high glucose, PAA Laboratories GmbH, Pasching, Austria), 10% FCS (Invitrogen GmbH, Darmstadt, Germany) and 1% penicillin/streptomycin (PAA Laboratories GmbH, Pasching, Austria) at 37°C and 5% CO₂ for 14 days. Two days after seeding, all non-adherent cells are removed by two washing steps with PBS.

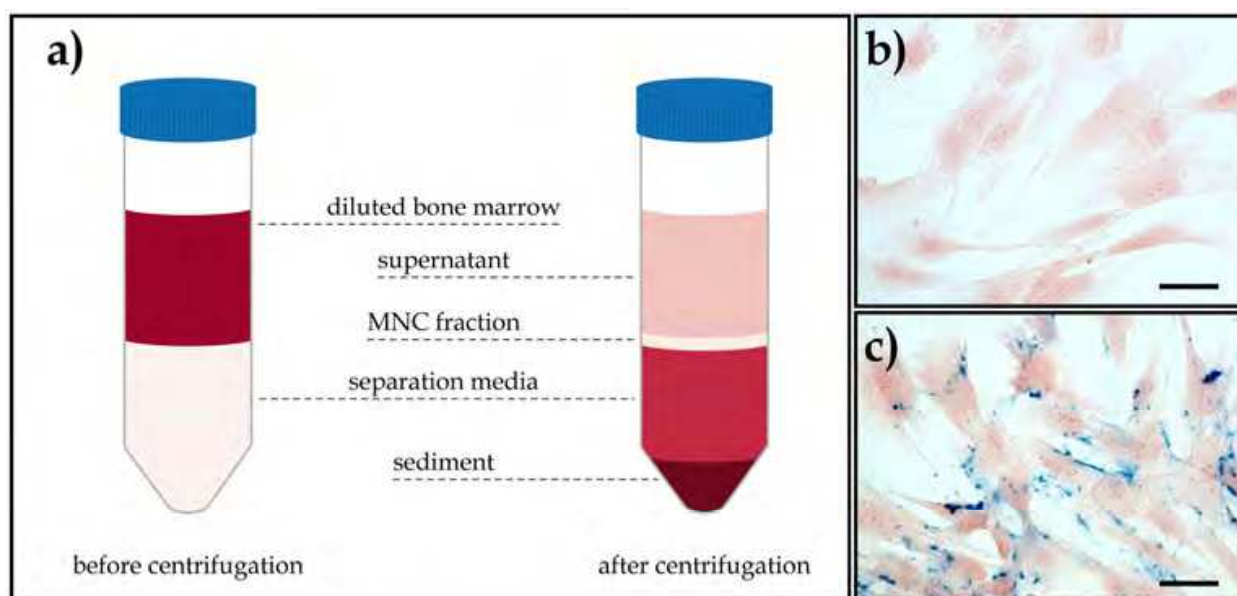


Fig. 8. Density gradient centrifugation of bone marrow and Prussian Blue staining of BMSC
a) Density gradient centrifugation of diluted bone marrow: segmentation before and after centrifugation (supernatant: serum and platelets, sediment: erythrocytes and granulocytes) is displayed; b) cultivated, unlabeled, ovine BMSC stained with Prussian Blue (PB) and eosin; c) VSOP-labeled BMSC stained with PB and eosin; scale bar: 50 μm

Cell labeling

Very small superparamagnetic iron oxide particles (VSOP, Ferropharm, Teltow, Germany) are used for magnetic cell labeling. VSOP consist of a 5 nm iron oxide core coated by monomer citrate (total diameter of 9 nm) with a negative surface charge. Iron particle incorporation by the cells causes a strong decrease in the transverse relaxation time, which results in signal loss in T₂*-weighted MR imaging (Arbab et al., 2003; Bowen et al., 2002; Renshaw et al., 1986). No apparent long-term cytotoxic effects were observed after using the particles both in vitro and in vivo (Fleige et al., 2002; Stroh et al., 2004 and 2009). For magnetic labeling sterile VSOP are added to the incubation medium. Addition of lipofection agents is not required for BMSC labeling. Cells are incubated with VSOP at 37°C and 5% CO₂ for 90 minutes. After incubation, the cells are washed three times with PBS to remove any remaining VSOP not endocytosed by cells. The cells are harvested by incubation with

trypsin (Invitrogen GmbH, Darmstadt, Germany) for 5 minutes and centrifugated at 350 x g. To visualize the incorporated iron oxide particles, Prussian Blue (PB) staining can be used (Fig. 8c). A protocol for PB staining is given in Table 1.

The cells can be labeled additionally using fluorescent dyes as GFP or PKH26, which may be helpful for histological examination after *in vivo* applications. This allows discrimination between initially labeled cells and cells that secondarily took up iron by endocytosis.

step	Prussian Blue staining	duration
1	Fixate in 4% paraformaldehyde	20 min
2	Stain with 2% potassium ferrocyanide, Trihydrate and 1% hydrochloride acid in a 1:1 ratio.	20 min
3	Wash in PBS	5 min
4	Stain in eosin	4 min
5	Wash in PBS	5 min
6	Conserve with glycerol (culture flasks) or mounting medium (slide)	

Table 1. Protocol for Prussian Blue staining of VSOP-labeled BMSC

Impact of VSOP labeling on cell viability and T2 relaxation time

The influence of 3.0 mM VSOP on cellular viability and magnetic labeling has been investigated for ovine BMSC in previous experiments. The viability was evaluated by the trypan blue dye exclusion test before labeling, immediately thereafter, as well as after 4 and 24 hours. Viability was compared to that of unlabeled cells. The transverse relaxation time (T2) was measured at 0.47 T/ 20 MHz (Minispec, Bruker, Ettlingen, Germany) immediately and 24 hours after VSOP-labeling to examine labeling efficacy.

Our own results show that cellular viability decreased to 86 ± 16 % immediately after labeling. At 4 hours after labeling, the cell viability rate remained unaltered (89 ± 14 %), but slightly declined to 75 ± 3 % after 24 hours (Fig. 9a). Relaxometry measurements resulted in T2 relaxation times of $1,888 \pm 171$ ms for unlabeled cells as compared to 434 ± 147 ms for VSOP-labeled cells ($p < 0.01$), indicating a reduction of T2-time to 23 ± 8 % after VSOP labeling (Fig. 9b, white). This result was reproduced 24 hours after labeling (Fig. 9b, black).

4.1.2 BMSC detection *in vivo*

Since VSOP shorten T2 relaxation time, the particles can be detected by MRI using gradient echo sequences, in particular T2* weighted imaging. Alternatively, susceptibility weighted imaging (SWI) can be used. The main difference to T2* is the inclusion of phase information into the image acquisition (Haacke et al., 2009). This is of particular advantage in case that dephasing particles such as iron-oxide particles are present in the respective voxel. The dephasing results in a hypointense signal at a given echo time. However, this signal loss is not specific, as there are a multitude of other sources of signal voids, such as blood and air.

The blooming effect is a well known phenomenon caused by iron oxide particles. Due to the augmented dephasing of proton spins, a major susceptibility artefact is depicted that exceeds the real dimension of the particle by a factor of up to 50. Hence, a small amount of

particles or labeled cells, or even single cells, can be detected by high field MRI (Dodd et al., 1999; Shapiro et al., 2005) taking advantage of the blooming effect.

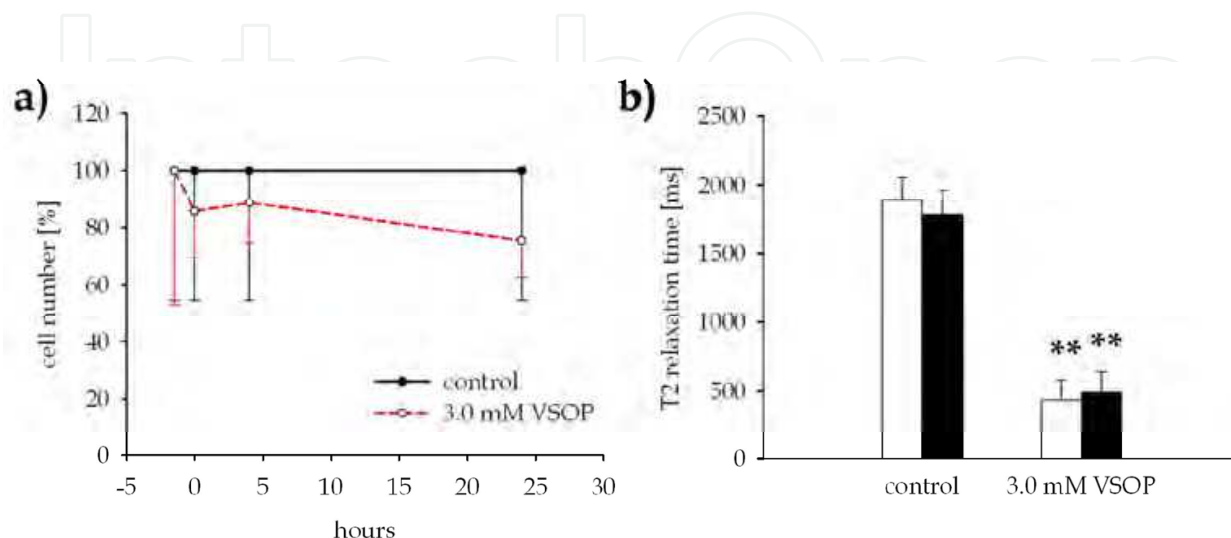


Fig. 9. Viability and relaxometry of VSOP-labeled BMSC

a) Viability during 24 hours after labeling, control treatment is set to 100%; b) Relaxometry of labeled and unlabeled BMSC. White bars: immediately; black bars: 24 hours after labeling (n=6 in each experiment)", **p<0.01.

sequence	resolution	TR	TE	duration
T2*	0.83 x 0.66 x 0.50 mm	620	20	2 h 07 min
SWI	0.56 x 0.39 x 0.25 mm	60	20	1h 29 min

Table 2. Parameters of MR imaging for detection of VSOP-labeled cells in ovine brain; TR - repetition time, TE - echo time

For in vivo detection of VSOP-labeled BMSC in the ovine brain a 3T MRI scanner (Magnetom Trio, Siemens AG, Munich, Germany) was used. After initial anesthesia the sheep was placed on the scanner table as described in 3.1.1 and shown in Fig. 10a. A flexible head coil (Siemens AG, Munich, Germany) was placed centrally above the brain (Fig. 10b). After a brief T2-weighted Turbo Spin Echo (TSE) sequence for anatomical orientation, SWI- and T2*-sequences were acquired with the field of view set to the region of transplantation. The sequence parameters are listed in Table 2. Two hours after transplantation, a distinct, ellipsoidal to circular hypointensity was detectable at all injection sites in T2* and SWI sequences (Fig. 11). This was not the case for control (saline) application without cells.

Histological examination allows discrimination of cellular signals to other sources of hypointense signal change (4.1.3).

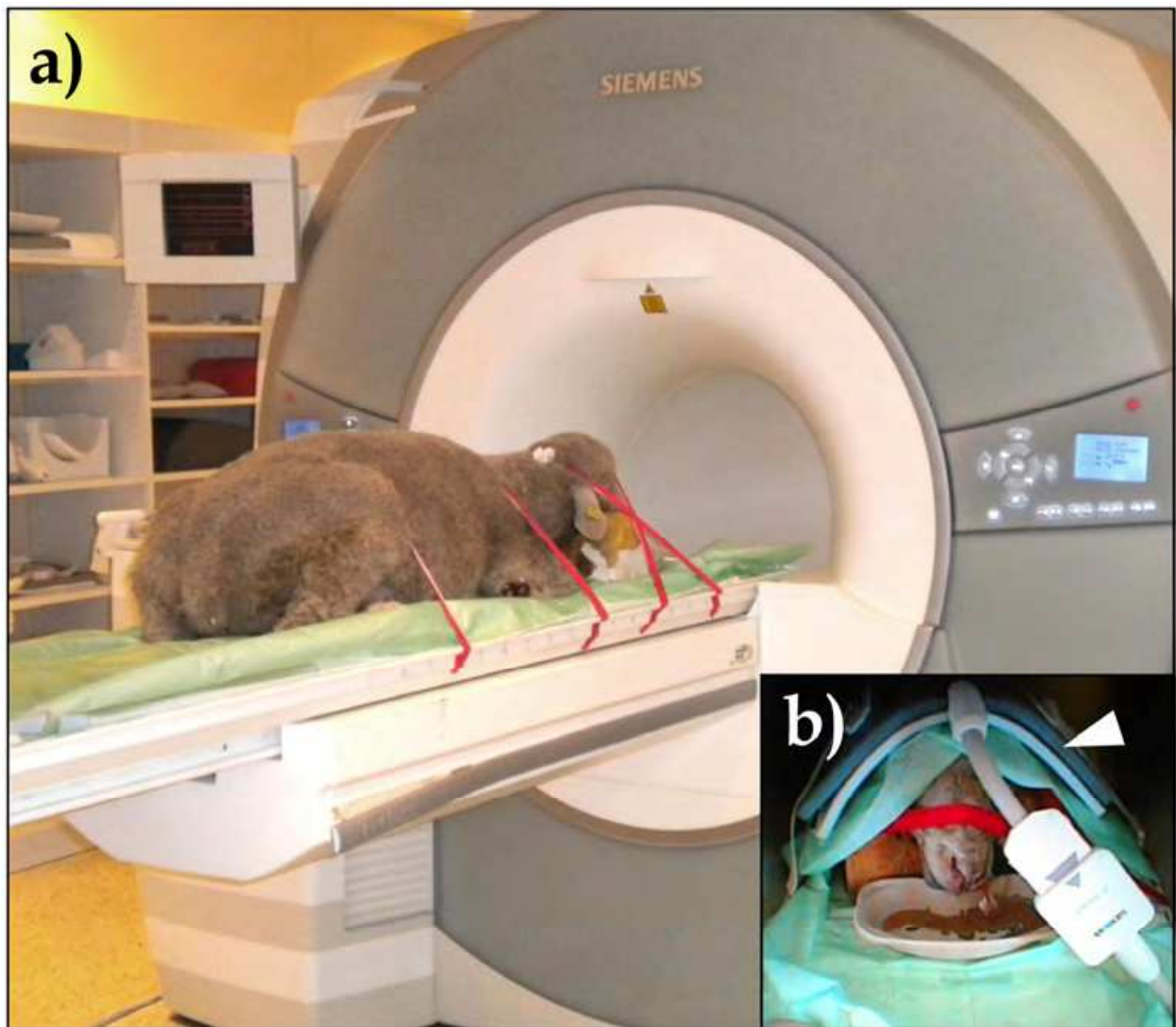


Fig. 10. MRI of sheep

a) Position of sheep in MR scanner. The animal is fixed with adhesive tap;
 b) Image taken by the scanner's monitoring camera. The head is placed on a position pad and covered with folio drape and a flexible head coil is used (white arrow). Potentially excreted saliva and rumen fluid are collected by a plastic bowl placed directly below the animal's mouth

The non-invasive detection of the transplanted cells allows longitudinal studies for up to six months in the individual animal for precise detection of migration and localization of transplanted cells (Jendelova et al., 2004; Stroh et al., 2004 and 2005). It can also be combined with stroke related MR-examinations and allows tracing of migration processes towards the lesion.

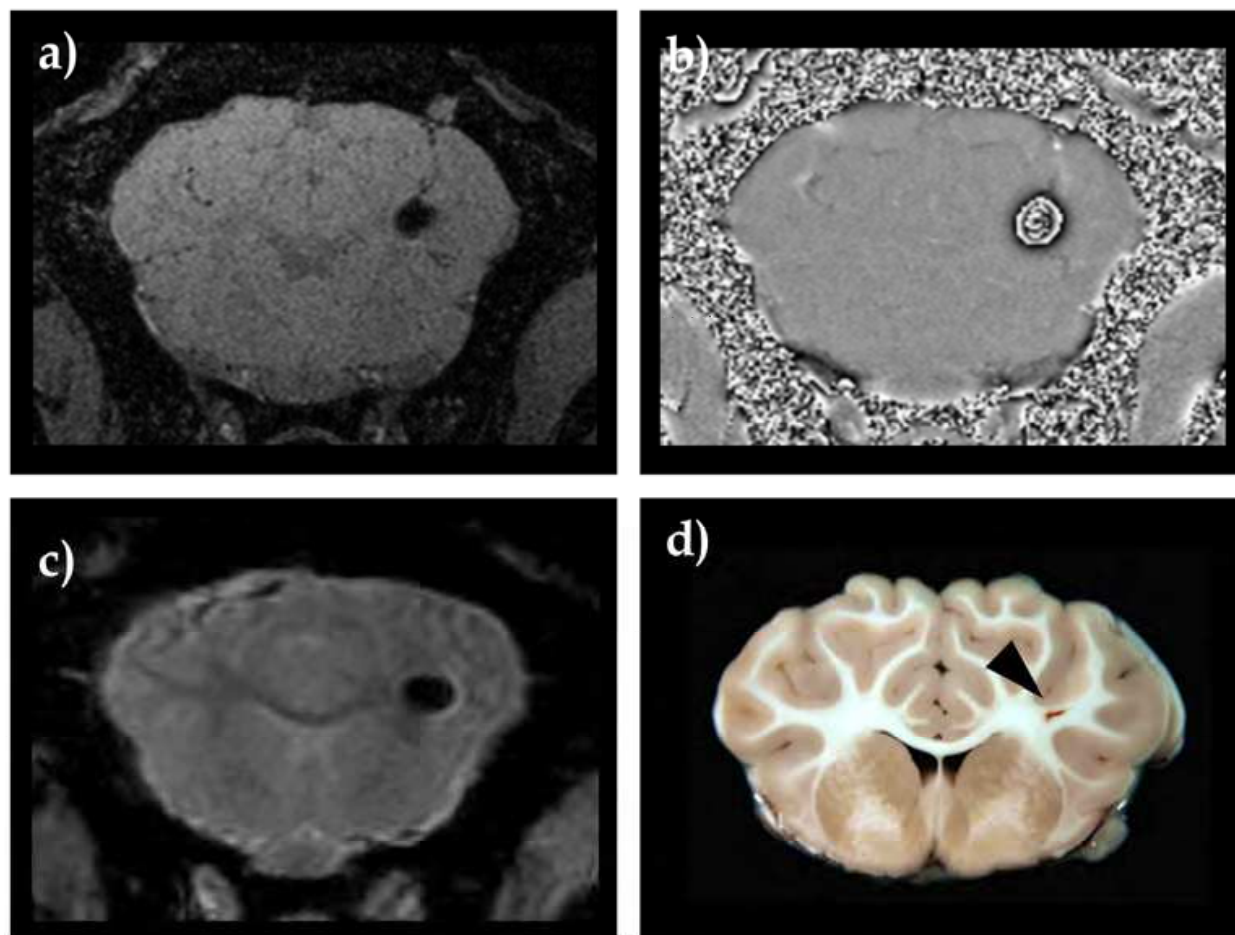


Fig. 11. MR and macroscopic view of 100,000 VSOP-labeled BMSC in the ovine brain a) susceptibility weighted imaging (SWI), b) phase image of SWI, c) T2* image, d) macroscopic view on brain slice. Black arrow indicates the macroscopically visible BMSC graft

4.1.3 Neuropathology and ex vivo BMSC detection

Animals are sacrificed during deep anesthesia by a single, intravenously injection of 20 mL pentobarbital (Eutha 77, Essex Pharma Ltd, Munich, Germany). After death is confirmed (absence of cardiac, respiratory and reflexive activity over a period of at least two minutes) the sheep is rapidly decapitated at the atlanto-occipital junction. The carotid arteries are exposed for perfusion. Blunt perfusion cannulas are placed in each artery and are fixed with stout thread. Initially, the head is perfused with 3 L PBS followed by 20 L 4% paraformaldehyde (PFA, Carl Roth GmbH & Co. KG, Karlsruhe, Germany). A roller pump system (Roth Cyclo II, Carl Roth GmbH & Co. KG, Karlsruhe, Germany) can be used for that purpose. After removal of skin, muscles and adnexes by a sharp knife, the cranial cavity is opened using an oscillating saw (KM-40, Heraeus GmbH, Hanau, Germany). After careful removal of the dura, the open cranium is fixated in 4% PFA for at least 24 hours. Afterwards, the brain is removed for immersion fixation for another 48 hours in PFA. Macroscopic examination of the brain comprises weighing, measuring of circumferences, and photographic documentation from all directions. Next, the brain is cut into 4 mm thick, coronal slices which are each photographed from rostral and occipital direction.

Usually, the transplantation procedure does not result in macroscopically visible brain tissue alterations. In a minor number of cases, a very small alteration is observable at the injection site (Fig. 12).

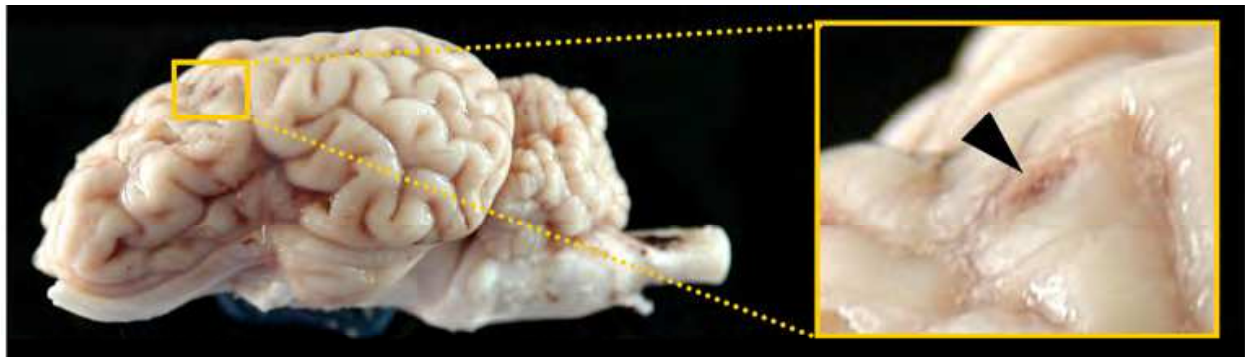


Fig. 12. Ovine brain after stereotatic transplantation

The insertion of the cannula may lead to a small alteration (black arrow) on the brain surface.

The transplantation area is cut out of the associated brain slice, embedded in paraffin and cut into 4 μm thick sections for histological analysis. Hematoxylin/eosin staining according to Table 3 is recommended for histological overview and exclusion of bleeding. Prussian Blue staining (according to Table 1, step 2 - 6) is used for detection of VSOP-labeled cells.

step	hematoxylin/eosin staining	duration
1	Stain in hematoxylin	2 min
2	Wash in piped water	2 min
3	Blue in warm piped water	10 min
4	Stain in eosin	4 min
5	Wash in pure water	5 min
6	Conservation (dehydrating, mounting)	

Table 3. Protocol for hematoxylin/eosin staining

Transplantation of 100,000 VSOP-labeled cells results in a brown spot at the transplantation site which was clearly visible in the coronal slice (Fig. 11d). Transplantation of PBS reveals no changes in the macroscopic view.

Histological investigation by hematoxylin/eosin staining usually reveals a small cavity containing the labeled cells with scattered mononuclear cells within the transplantation site 8 hours after transplantation. Occasionally, microbleedings may occur close to the injection site. In sheep transplanted with VSOP-labeled BMSC, PB-positive cells are clearly detected at the specified target region (Fig. 13). No migration of cells is observed 8 hours after transplantation.

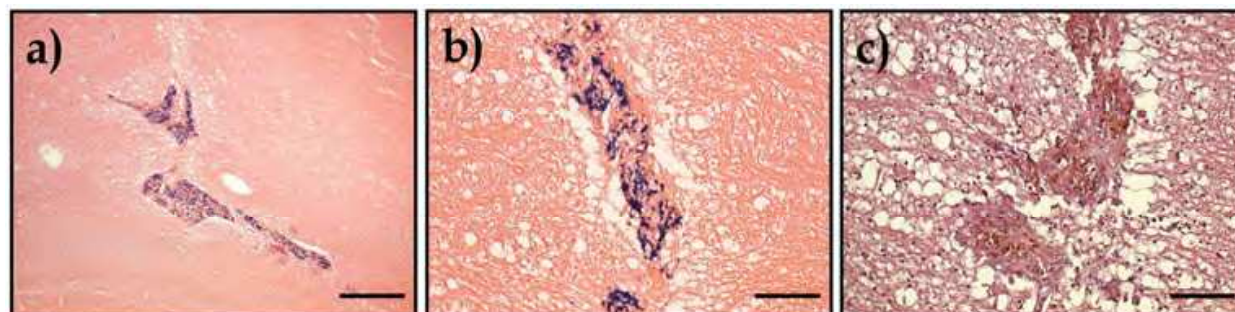


Fig. 13. Histological analysis of 100,000 transplanted, VSOP-labeled BMSC after striatal application

a) Overview of transplantation site stained with PB, scale bar: 500 μm ; b) Magnification of PB staining, scale bar: 100 μm ; c) hematoxylin/eosin staining of transplantation site, no microhemorrhages (e.g. due to cell injection) are detectable; bar: 100 μm

4.2 Concept 2: Hemorrhage model

4.2.1 Hemorrhage detection

T1-, T2- and T2*-weighted MR sequences can be used for hemorrhage detection. The injection of autologous blood into the sheep brain usually results in a spheric to ellipsoid-shaped blood clot, with the depot size depending on the injected blood volume. The MR signal characteristics of the hemorrhage differ depending on the temporal stage of the hemorrhage and the pulse sequence used (Kidwell & Wintermark, 2008). In the hyperacute stage, hemoglobin is still oxygenated and therefore diamagnetic, thus appearing iso- to hypointense in T1-weighted sequences (Fig. 14a) and hyperintense in T2-weighted MRI (Fig. 15a). A hypointense rim is observable in T2* sequence (Fig. 14b and c). In contrast, methemoglobin is present in the sub-acute stage. Methemoglobin is paramagnetic and generates a hyperintensive signal in T1-weighted and a hypointensive signal in T2-weighted MRI. Later, the signal changes become hypointensive in T1- and T2-weighted MRI due to the progressive biodegradation of hemoglobin into superparamagnetic hemosiderin

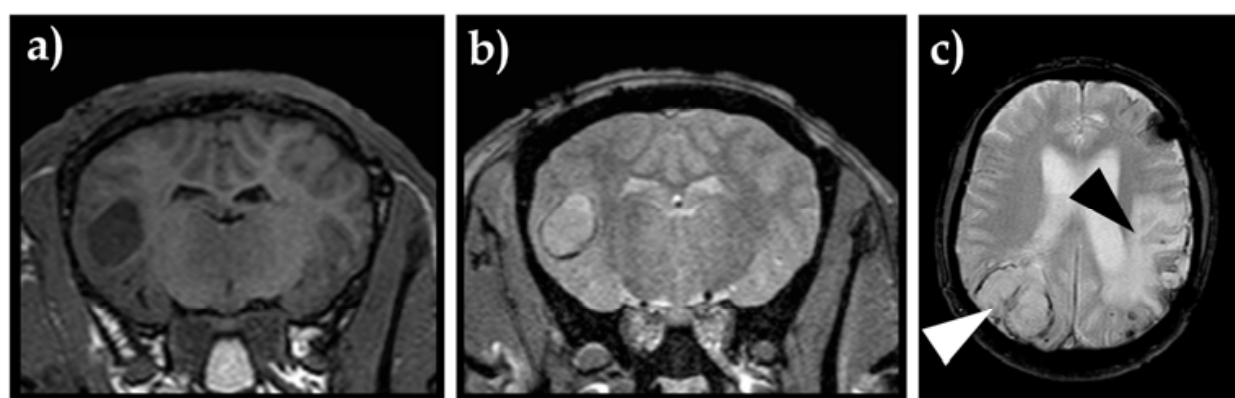


Fig. 14. Imaging of stereotactically placed blood clot (1.8 mL, 3 hours old) in ovine brain for simulation of intracerebral hemorrhage using T1 weighted (a) and T2* weighted sequences (b). An acute occipital intracerebral bleed in a human patient (T2*, 2 hours after onset of visual disturbances, white arrow) is shown in c) for direct comparison. For more details, please refer to main text. Note an old left temporal ischemia (secondary diagnosis) in this particular patient (black arrow)

towards the chronic phase of a hemorrhage. Also, a blooming effect can be observed by the high iron oxide content of hemosiderin (4.1.2).

Fig. 14 gives a direct comparison between a stereotactically injected blood depot in the sheep model and a hyperacute bleeding in a human patient (with symptom onset of approx. 2 h before MRI) in T2* MRI. A hyperintense signal is clearly observable in the center of the injected blood in the sheep brain (b) and the hyperacute intracerebral hemorrhage in the human patient (c), whereas a clear hypointense rim can be detected in the outer areas of the hemorrhage in both subjects. This difference in the signal intensity is caused by oxygenated hemoglobin in the central areas and deoxygenated hemoglobin in the peripheral areas of the hemorrhage. This signal behavior is typical for a hyperacute hemorrhage within a timeframe of approximately 3 to 9 h after symptom onset in human beings (Howells et al., 2010). In summary, the blood-induced MR signal 3 hours after autologous blood injection in the sheep model shows the same characteristics to the situation found in the human patient.

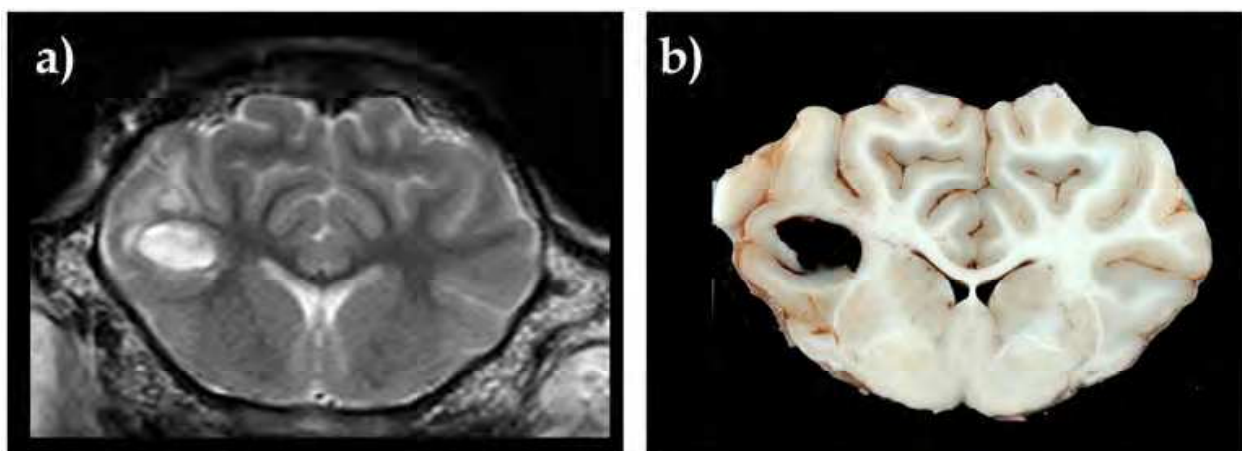


Fig. 15. MRI of induced, acute hemorrhage (1.5 mL) in the ovine brain
 a) T2-weighted TSE sequence with a clearly observable, hyperintensive area (blood clot),
 b) corresponding macroscopic view of brain slice

Tissue preparation for gross pathology after hemorrhage modeling can be performed according to 4.1.3. The clearly observable cavity in Fig. 15b indicates the injection site. The tissue around the injection site was compressed during blood injection. Similar findings are reported from autopsies of human patients who died from massive intracerebral hemorrhage in early stages.

5. Summary

Stereotactic neurosurgery is a routine technique in human medicine. Stereotaxy-based local treatments of stroke (and other diseases) were effectively tested in rodents using strain- and weight-adapted coordinates and approaches. Hence, it is expected that intracerebral administration paradigms will be evaluated in upcoming clinical trials. However, a proof of concept of such treatment paradigms may be demanded in translational research, preferentially using large animal models. However, similar techniques were so far only available for primate models which are restricted to highly specialized centers.

The described, frameless stereotaxy in sheep represents a novel and translational approach for neurosurgical applications in a widely available species. The used neuronavigation

system BrainSight™ was successfully adapted to the ovine skull anatomy. It allows an individual and accurate planning as well as precise execution of stereotactic interventions. Next to a detailed description of the technique itself, two relevant applications of the experimental techniques are reported in this chapter. First, the magnetic labeling and stereotactic transplantation of a stem cell population into the ovine brain is described. The methodology allows for precise injection and tracking of autologous stem cell populations using a widely available 3T MRI scanner. Relatively simple but reliable pathohistological techniques for post-mortem brain assessment and detection of transplanted cells are also given. Thus, the reported methodology may be used for evaluation of cell-based treatment strategies of central nervous system disorders in the gyrencephalic brain. Second, the stereotactic technique can be used for precise modeling of intracerebral hemorrhages by autologous blood injection in sheep. The observed results are in good correlation to those seen in human patients, especially regarding relevant diagnostic findings in MRI. Summarizing, stereotactic interventions in sheep represent a well applicable and reliable approach for translational research with a wide spectrum of possible applications.

6. Acknowledgment

The authors thank Dr. Stephen Frey from Rogue Research Inc. for technical support and the staff of the Institute of Anatomy, Histology and Embryology, Faculty of Veterinary Medicine, University of Leipzig.

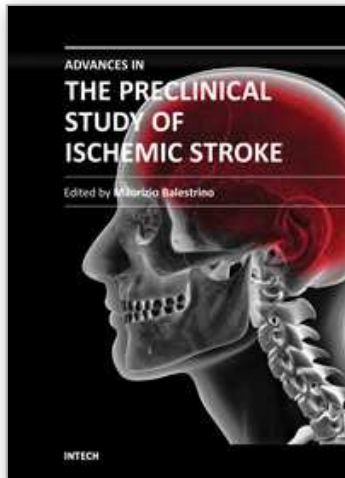
7. References

- Amiridze, N., Gullapalli, R., Hoffman, G. & Darwish, R. (2009). Experimental model of brainstem stroke in rabbits via endovascular occlusion of the basilar artery. *J Stroke Cerebrovasc Dis.*, 18,4,281-287
- Arbab, A.S., Bashaw, L.A., Miller, B.R., Jordan, E.K., Bulte, J.W. & Frank, J.A. (2003). Intracytoplasmic tagging of cells with ferumoxides and transfection agent for cellular magnetic resonance imaging after cell transplantation: methods and techniques. *Transplantation.*, 76, 7, 123-130
- Barber, P.A., Zhang, J., Demchuk, A.M., Hill, M.D. & Buchan, A.M. (2001). Why are stroke patients excluded from TPA therapy? An analysis of patient eligibility. *Neurology*, 56, 8, 1015-1020
- Blinzler, C., Breuer, L., Huttner, H.B., Schellinger, P.D., Schwab, S. & Köhrmann, M. (2011). Characteristics and outcome of patients with early complete neurological recovery after thrombolysis for acute ischemic stroke. *Cerebrovasc Dis.*, 31, 2, 185-190
- Boltze, J., Förchler, A., Nitzsche, B., Waldmin, D., Hoffmann, A., Boltze, C.M., Dreyer, A.Y., Goldammer, A., Reischauer, A., Härtig, W., Geiger, K.D., Barthel, H., Emmrich, F. & Gille, U. (2008). Permanent middle cerebral artery occlusion in sheep: a novel large animal model of focal cerebral ischemia. *J Cereb Blood Flow Metab.*, 28, 12, 1951-1964
- Bowen, C.V., Zhang, X., Saab, G., Gareau, P.J. & Rutt, B.K. (2002). Application of the static dephasing regime theory to superparamagnetic iron-oxide loaded cells. *Magn Reson Med.*, 48, 1, 52-61

- Bullock, R., Mendelow, A.D., Teasdale, G.M. & Graham, D.I. (1984). Intracranial haemorrhage induced at arterial pressure in the rat. Part 1: Description of technique, ICP changes and neuropathological findings. *Neurol Res.*, 6, 4, 184-188
- Burns, T.C. & Steinberg, G.K. (2011). Stem cells and stroke: opportunities, challenges and strategies. *Expert Opin Biol Ther.*, 11, 4, 447-461
- Del Zoppo, G.J. (1995). Why do all drugs work in animals but none in stroke patients? 1. Drugs promoting cerebral blood flow. *J Intern Med.*, 237, 1, 79-88
- Dodd, S.J., Williams, M., Suhan, J.P., Williams, D.S., Koretsky, A.P. & Ho, C. (1999). Detection of single mammalian cells by high-resolution magnetic resonance imaging. *Biophys J.*, 76, 1 Pt 1, 103-109
- Fisher, M., Feuerstein, G., Howells, D.W., Hurn, P.D., Kent, T.A., Savitz, S.I., Lo, E.H. & STAIR Group. (2009). Update of the stroke therapy academic industry roundtable preclinical recommendations. *Stroke*, 40, 6, 2244-2250
- Fleige, G., Seeberger, F., Laux, D., Kresse, M., Taupitz, M., Pilgrim, H. & Zimmer, C. (2002). In vitro characterization of two different ultrasmall iron oxide particles for magnetic resonance cell tracking. *Invest Radio.l.*, 37, 9, 482-488
- Flower, O. & Smith, M. (2011). The acute management of intracerebral hemorrhage. *Curr Opin Crit Care.*, 17, 2, 106-114
- Frey, S., Comeau, R., Hynes, B., Mackey, S. & Petrides, M. (2004). Frameless stereotaxy in the nonhuman primate. *Neuroimage*, 23, 3, 1226-1234
- Garcia, J.H., Kalimo, H., Kamijyo, Y. & Trump, B.F. (1977). Cellular events during partial cerebral ischemia. I. Electron microscopy of feline cerebral cortex after middle-cerebral-artery occlusion. *Virchows Arch B Cell Pathol.*, 25, 3, 191-206
- Gross, R.E., Watts, R.L., Hauser, R.A., Bakay, R.A., Reichmann, H., von Kummer, R., Ondo, W.G., Reissig, E., Eisner, W., Steiner-Schulze, H., Siedentop, H., Fichte, K., Hong, W., Cornfeldt, M., Beebe, K., Sandbrink, R. & Spheramine Investigational Group. (2011). Intraatrial transplantation of microcarrier-bound human retinal pigment epithelial cells versus sham surgery in patients with advanced Parkinson's disease: a double-blind, randomised, controlled trial. *Lancet Neurol.*, 10, 6, 509-519
- Guzman, R., Uchida, N., Bliss, T.M., He, D., Christopherson, K.K., Stellwagen, D., Capela, A., Greve, J., Malenko, R.C., Mosley, M.E., Palmer, T.D. & Steinberg, G.K. (2007). Long-term monitoring of transplanted human neural stem cells in developmental and pathological contexts with MRI. *Proc Natl Acad Sci U S A*, 104, 24, 10211-10216
- Haacke, E.M., Mittal, S., Wu, Z., Neelavalli, J. & Cheng, Y.C. (2009). Susceptibility-weighted imaging: technical aspects and clinical applications, part 1. *AJNR Am J Neuroradiol.*, 30, 1, 19-30
- Hacke, W., Kaste, M., Bluhmki, E., Brozman, M., Dávalos, A., Guidetti, D., Larrue, V., Lees, K.R., Medeghri, Z., Machnig, T., Schneider, D., von Kummer, R., Wahlgren, N., Toni, D. & ECASS Investigators (2008). Thrombolysis with alteplase 3 to 4.5 hours after acute ischemic stroke. *N Engl J Med.*, 359, 13, 1317-1329
- Hoehn, M., Kustermann, E., Blunk, J., Wiedermann, D., Trapp, T., Wecker, S., Föcking, M., Arnold, H., Heschler, J., Fleischmann, B.K., Schwind, W. & Bührle, C. (2002). Monitoring of implanted stem cell migration in vivo: a highly resolved in vivo magnetic resonance imaging investigation of experimental stroke in rat. *Proc Natl Acad Sci U S A*, 99, 25, 16267-16272

- Howells, D.W., Porritt, M.J., Rewell, S.S., O'Collins, V., Sena, E.S., van der Worp, H.B., Traystman, R.J. & Macleod, M.R. (2010). Different strokes for different folks: the rich diversity of animal models of focal cerebral ischemia. *J Cereb Blood Flow Metab.*, 30, 8, 1412-1431
- Imai, H., Konno, K., Nakamura, M., Shimizu, T., Kubota, C., Seki, K., Honda, F., Tomizawa, S., Tanaka, Y., Hata, H. & Saito, N. (2006). A new model of focal cerebral ischemia in the miniature pig. *J Neurosurg.*, 104, 2, 123-132
- Jendelova, P., Herynek, V., Urdzikova, L., Glogarova, K., Kroupova, J., Andersson, B., Bryja, V., Burian, M., Hajek, M. & Sykova, E. (2004) Magnetic resonance tracking of transplanted bone marrow and embryonic stem cells labeled by iron oxide nanoparticles in rat brain and spinal cord. *J Neurosci Res.*, 76, 2, 232-243
- Joyce, N., Annett, G., Wirthlin, L., Olson, S., Bauer, G. & Nolte, J.A. (2010) Mesenchymal stem cells for the treatment of neurodegenerative disease. *Regen Med.*, 5, 6, 933-946
- Kang, B.T., Lee, J.H., Jung, D.I., Park, C., Gu, S.H., Jeon, H.W., Jang, D.P., Lim, C.Y., Quan, F.S., Kim, Y.B., Cho, Z.H., Woo, E.J. & Park, H.M. (2007). Canine model of ischemic stroke with permanent middle cerebral artery occlusion: clinical and histopathological findings. *J Vet Sci.*, 8, 4, 369-376
- Kidwell, C.S. & Wintermark, M. (2008). Imaging of intracranial haemorrhage. *Lancet Neurol.*, 7, 3, 256-267
- Klintworth, G.K. (1965). The pathogenesis of secondary brainstem hemorrhages as studied in an experimental model. *Am J Pathol.*, 47, 4, 525-536
- Kolominsky-Rabas, P.L., Heuschmann, P.U., Marschall, D., Emmert, M., Baltzer, N., Neundörfer, B., Schöffski, O. & Krobot, K.J. (2006). Lifetime cost of ischemic stroke in Germany: results and national projections from a population-based stroke registry: the Erlangen Stroke Project. *Stroke*, 37, 5, 1179-1183
- Kondziolka, D., Steinberg, G.K., Wechsler, L., Meltzer, C.C., Elder, E., Gebel, J., Decesare, S., Jovin, T., Zafonte, R., Lebowitz, J., Flickinger, J.C., Tong, D., Marks, M.P., Jamieson, C., Luu, D., Bell-Stephens, T. & Teraoka, J. (2005). Neurotransplantation for patients with subcortical motor stroke: a phase 2 randomized trial. *J Neurosurg.*, 103, 1, 38-45
- Lansberg, M.G., Schrooten, M., Bluhmki, E., Thijs, V.N. & Saver, J.L. (2009). Treatment time-specific number needed to treat estimates for tissue plasminogen activator therapy in acute stroke based on shifts over the entire range of the modified Rankin Scale. *Stroke*, 40, 6, 2079-2084
- MacLellan, C.L., Silasi, G., Auriat, A.M. & Colbourne, F. (2010). Rodent models of intracerebral hemorrhage. *Stroke*, 41, 10, 95-98
- Natarajan, S.K., Snyder, K.V., Siddiqui, A.H., Ionita, C.C., Hopkins, L.N. & Levy, E.I. (2009). Safety and effectiveness of endovascular therapy after 8 hours of acute ischemic stroke onset and wake-up strokes. *Stroke*, 40, 10, 3269-3274
- O'Collins, V.E., Macleod, M.R., Donnan, G.A., Horvath, L.L., van der Worp, B.H. & Howells, D.W. (2006). 1,026 experimental treatments in acute stroke. *Ann Neurol.*, 59, 3, 467-477
- Olivier, A., Bertrand, G. (1983). A new head clamp for stereotactic and intracranial procedures. Technical note. *Appl. Neurophysiol.*, 46, 5-6, 272-275
- Renshaw, P.F., Owen, C.S., McLaughlin, A.C., Frey, T.G. & Leigh, J.S., Jr. (1986). Ferromagnetic contrast agents: a new approach. *Magn Reson Med.*, 3, 2, 217-225
- Rymer, M.M. (2011). Hemorrhagic stroke: intracerebral hemorrhage. *Mo Med.*, 108, 1, 50-54

- Sahota, P. & Savitz, S.I. (2011). Investigational therapies for ischemic stroke: neuroprotection and neurorecovery. *Neurotherapeutics*, 8, 3, 434-451
- Samadani, U. & Rohde, V. (2009). A review of stereotaxy and lysis for intracranial hemorrhage. *Neurosurg Rev.*, 32, 1, 15-22
- Savitz, S.I., Chopp, M., Deans, R., Carmichael, S.T., Phinney, D. & Wechsler, L. (2011). Stem Cell Therapy as an Emerging Paradigm for Stroke (STEPS) II. *Stroke*, 42, 3, 825-829
- Shapiro, E.M., Skrtic, S. & Koretsky, A.P. (2005). Sizing it up: cellular MRI using micron-sized iron oxide particles. *Magn Reson Med.*, 53, 2, 329-338
- Shobha, N., Buchan, A.M., Hill, M.D. & Canadian Alteplase for Stroke Effectiveness Study (CASES) (2011). Thrombolysis at 3-4.5 hours after acute ischemic stroke onset--evidence from the Canadian Alteplase for Stroke Effectiveness Study (CASES) registry. *Cerebrovasc Dis.*, 31, 3, 223-228
- Stadler, J.A. 3rd, Ellens, D.J. & Rosenow, J.M. (2011). Deep brain stimulation and motor cortical stimulation for neuropathic pain. *Curr Pain Headache Rep.*, 15, 1, 8-13.
- Starr, P.A., Vitek, J.L. & Bakay, R.A. (1998). Ablative surgery and deep brain stimulation for Parkinson's disease. *Neurosurgery*, 43, 5, 989-1013
- Stroh, A., Zimmer, C., Gutzeit, C., Jakstadt, M., Marschinke, F., Jung, T., , Pilgrimm, H. & Grune, T. (2004). Iron oxide particles for molecular magnetic resonance imaging cause transient oxidative stress in rat macrophages. *Free Radic Biol Med.*, 36, 8, 976-984
- Stroh, A., Faber, C., Neuberger, T., Lorenz, P., Sieland, K., Jakob, P.M., Webb, A., Pilgrimm, H., Schober, R., Pohl, E.E. & Zimmer, C. (2005). In vivo detection limits of magnetically labeled embryonic stem cells in the rat brain using high-field (17.6 T) magnetic resonance imaging. *Neuroimage*, 24, 3, 635-645
- Stroh, A., Boltze, J., Sieland, K., Hild, K., Gutzeit, C., Jung, T., Kressel, J., Hau, S., Reich, D., Grune, T. & Zimmer, C. (2009). Impact of magnetic labeling on human and mouse stem cells and their long-term magnetic resonance tracking in a rat model of Parkinson disease. *Mol Imaging*, 8, 3, 166-178
- The STAIR Participants. (1999). Recommendations for standards regarding preclinical neuroprotective and restorative drug development. *Stroke*, 30, 12, 2752-2758
- The STEPS Participants. (2009) Stem Cell Therapies as an Emerging Paradigm in Stroke (STEPS): bridging basic and clinical science for cellular and neurogenic factor therapy in treating stroke. *Stroke*, 40, 2, 510-515
- Willems, P.W., van der Sprenkel, J.W., Tulleken, C.A., Viergever, M.A. & Taphoorn, M.J. (2006). Neuronavigation and surgery of intracerebral tumours. *J Neurol.*, 253, 9, 1123-1136
- Zhu, H., Li, Q., Feng, M., Chen, Y.X., Li, H., Sun, J.J., Zhao, C.H., Wang, R.Z., Bezard, E. & Qin, C. (2011). A new cerebral hemorrhage model in cynomolgus macaques created by injection of autologous anticoagulated blood into the brain. *J Clin Neurosci.*, 18, 7, 955-960



Advances in the Preclinical Study of Ischemic Stroke

Edited by Dr. Maurizio Balestrino

ISBN 978-953-51-0290-8

Hard cover, 530 pages

Publisher InTech

Published online 16, March, 2012

Published in print edition March, 2012

This book reports innovations in the preclinical study of stroke, including - novel tools and findings in animal models of stroke, - novel biochemical mechanisms through which ischemic damage may be both generated and limited, - novel pathways to neuroprotection. Although hypothermia has been so far the sole "neuroprotection" treatment that has survived the translation from preclinical to clinical studies, progress in both preclinical studies and in the design of clinical trials will hopefully provide more and better treatments for ischemic stroke. This book aims at providing the preclinical scientist with innovative knowledge and tools to investigate novel mechanisms of, and treatments for, ischemic brain damage.

How to reference

In order to correctly reference this scholarly work, feel free to copy and paste the following:

Antje Dreyer, Albrecht Stroh, Claudia Pösel, Matthias Findeisen, Teresa von Geymüller, Donald Lobsien, Björn Nitzsche and Johannes Boltze (2012). Frameless Stereotaxy in Sheep - Neurosurgical and Imaging Techniques for Translational Stroke Research, *Advances in the Preclinical Study of Ischemic Stroke*, Dr. Maurizio Balestrino (Ed.), ISBN: 978-953-51-0290-8, InTech, Available from: <http://www.intechopen.com/books/advances-in-the-preclinical-study-of-ischemic-stroke/frameless-stereotaxy-in-sheep-neurosurgical-and-imaging-techniques-for-translational-stroke-research>

INTECH
open science | open minds

InTech Europe

University Campus STeP Ri
Slavka Krautzeka 83/A
51000 Rijeka, Croatia
Phone: +385 (51) 770 447
Fax: +385 (51) 686 166
www.intechopen.com

InTech China

Unit 405, Office Block, Hotel Equatorial Shanghai
No.65, Yan An Road (West), Shanghai, 200040, China
中国上海市延安西路65号上海国际贵都大饭店办公楼405单元
Phone: +86-21-62489820
Fax: +86-21-62489821

© 2012 The Author(s). Licensee IntechOpen. This is an open access article distributed under the terms of the [Creative Commons Attribution 3.0 License](#), which permits unrestricted use, distribution, and reproduction in any medium, provided the original work is properly cited.

IntechOpen

IntechOpen